Available online at www.sciencedirect.com
ScienceDirect
Solid-State Electronics 51 (2007) 757–761
SOLID-STATE ELECTRONICS
www.elsevier.com/locate/sse

# Ultraviolet photoconductive detector with high visible rejection and fast photoresponse based on ZnO thin film

K.W. Liu [a,b,*], J.G. Ma [a], J.Y. Zhang [a], Y.M. Lu [a], D.Y. Jiang [a,b], B.H. Li [a], D.X. Zhao [a], Z.Z. Zhang [a], B. Yao [a], D.Z. Shen [a]

[a] *Key Laboratory of Excited State Processes, Changchun Institute of Optics, Fine Mechanics and Physics, Chinese Academy of Sciences, 16-Dongnanhu Road, Changchun 130033, China*
[b] *Graduate School of the Chinese Academy of Sciences, Beijing 100049, China*

Received 21 September 2006; received in revised form 1 March 2007; accepted 5 March 2007
Available online 26 April 2007

The review of this paper was arranged by Prof. Y. Arakawa

**Abstract**

In this study, metal–semiconductor–metal (MSM) photoconductive detector was fabricated on *c*-axis preferred oriented ZnO film prepared on quartz by radio frequency magnetron sputtering. With the applied bias below 3 V, the dark current was below 250 nA. The typical responsivity peaked at around 360 nm, and had values of 30 A/W. In addition, the UV (360 nm) to visible (450 nm) rejection ratio of around five orders could be extracted from the spectra response. Furthermore, the transient response measurement revealed fast photoresponse with a rise time of 20 ns.


*Keywords:* ZnO; MSM; Photoconductive detector; Responsivity

## 1. Introduction

Ultraviolet (UV) photodetector has drawn a great deal of interest in recent years, due to their potential application such as solar astronomy, missile plume detection, space-to-space transmission, fire alarm and combustion monitoring [1–4]. As a direct wide band gap ($E_g = 3.3$ eV) semiconductor, ZnO can be used for UV photon detection. Its high radiation hardness enables it to be used in harsh environments [5]. The availability of lattice-matched single crystal ZnO substrates and the relatively low deposition temperatures (100–750 °C) ease the device processing [6]. Owing to its large exciton binding energy (~60 meV), ZnO has attracted increasing attention in recent years for potential low threshold blue/UV lasers that can be integrated with photodetectors [7]. However, the lack of reliable p-type ZnO hinders any p–n junction based optoelectronic devices [8]. The reports of ZnO–UV detectors mainly focus on metal–semiconductor–metal (MSM) structure which contains either Schottky-barrier-based photovoltage type or ohmic contact based photoconductive type [9–13,10,14,15]. Among them, the photoconductive detector is easy to obtain higher gain and photoresponsivity, so the amplifying equipment is not necessary and the measuring system is simple and cheap. However, this gain is associated with a nonlinear behaviour with incident power, poor UV/visible contrast, and persistent photoconductivity effects [16]. Furthermore, the photoresponse time of photoconductive detector is usually longer than other types for the persistent photoconductivity. According to the early report, both

* Corresponding author. Address: Key Laboratory of Excited State Processes, Changchun Institute of Optics, Fine Mechanics and Physics, Chinese Academy of Sciences, 16-Dongnanhu Road, Changchun 130033, China. Tel.: +86 431 6176322.
*E-mail address:* liukewei23@sohu.com (K.W. Liu).

0038-1101/$ - see front matter © 2007 Elsevier Ltd. All rights reserved.
doi:10.1016/j.sse.2007.03.002

linearly and visible rejection can be considerably improved by using a lock-in detection system [17]. Meanwhile, the reported photoresponse time of ZnO photoconductive UV detector is equal or above 0.1 μs [11,12,10] and this drawback makes the photoconductor unsuitable for application in circumstances of high-speed photoresponse. So it is important to improve the photoresponse time of the photoconductive detector due to which the photoconductor with fast rise time could be widely used in missile plume detection and alarm.

In this letter, we report on the epitaxial growth of *c*-preferred oriented ZnO film on quartz by radio frequency magnetron sputtering, as well as the fabrication and characterization of photoconductive ZnO MSM UV detectors. The advantage of growing ZnO films on quartz substrates is the low cost and it will open an avenue to realize UV detectors on flexible substrates as well. The detectors exhibited a long-wavelength cutoff at 380 nm and a high responsivity in the UV region with only a little decrease from 360 to 250 nm. The time response and voltage-dependent of responsivity were also measured and discussed.

## 2. Experiment

Radio frequency (rf) magnetron sputtering was used to grow ZnO layer on $SiO_2$ substrate. Before sputtering, the substrates were cleaned by acetone and ethanol for 5 min in an ultrasonic bath, followed by a de-ionized water rinse. Highly pure Zn disk (90 mm in diameter and 10 mm in thickness) was used as sputtering target. The base pressure of sputtering chamber was evacuated to be below $3 \times 10^{-4}$ Pa with a turbo molecular pump. The target-substrate distance was maintained at 50 mm and the substrate temperature was controlled at 400 °C. The working pressure in the chamber was kept at 1.0 Pa during the film growth. The rf power was kept at 150 W. Ultrapure (5 N) Ar and $O_2$ gases were introduced into the sputtering chamber through a set of mass flow controllers with the flow rates of 60 and 20 SCCM (standard cubic centimeter per minute), respectively. The film thickness was 300 nm with the deposition rate of 6 nm/min.

Interdigitated Au ohmic metal contacts were deposited on the ZnO sample on quartz substrate by vacuum evaporation in order to fabricate the MSM photoconductive detector. Scanning electronic microscope picture of ZnO UV detector with MSM structure is shown in Fig. 1. The fingers were 500 μm long and 5μm wide with a pitch of 5 μm. The thickness of the Au electrodes is 200 nm. There are 12 pair fingers in the interdigitated structure.

A Ringaku O/max-RA X-ray diffractometer (XRD) with Cu Kα radiation ($\lambda = 0.154178$ nm) was used to make $\theta$–$2\theta$ scans to evaluate the crystalline property of ZnO. Both optical transmission and absorption spectra were recorded using a Shimadzu UV-3101PC scanning spectrophotometer. The dark current was measured by semiconductor parameter analyzer.

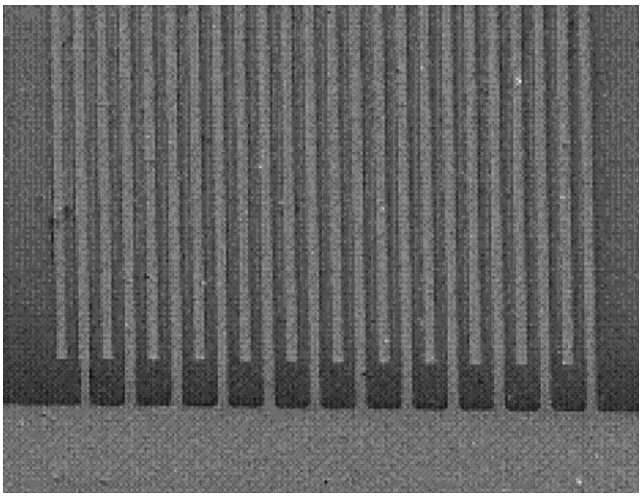

Fig. 1. Scanning electronic microscope picture of ZnO UV detector with MSM structure. The Au fingers are 500 μm long, 5 μm wide and have an interelectrode spacing of 5 μm.

## 3. Results and Discussion

Fig. 2 shows the XRD pattern of ZnO thin film prepared by radio frequency magnetron sputtering. Only the (0 0 2) diffraction peak at about 34.4° with the full width at half maximum (FWHM) of 0.6° could be found. Therefore, it is obvious that the film is *c*-axis preferred oriented.

Fig. 3 shows the transmission and absorption spectra of the film. The substrate contribution is excluded. Within the visible region, the average transmittance is more than 80%. The ZnO optical band gap obtained from the absorption spectrum is about 3.24 eV.

Shown in Fig. 4 are the dark and photoilluminated *I*–*V* characteristics of the ZnO MSM planar device. The wavelength and power of the illuminated light are 350 nm and 5 μW, respectively. Such a linear relation indicates the

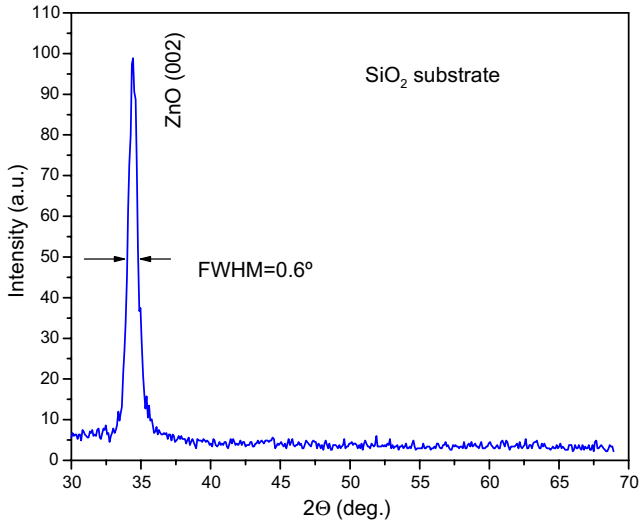


Fig. 2. XRD spectra of ZnO film prepared by rf magnetron sputtering on quartz at 400 °C.

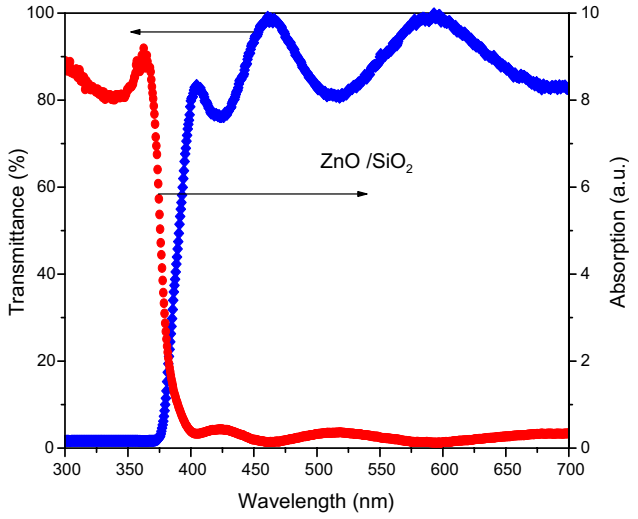


Fig. 3. UV–visible transmission and absorption spectrum of ZnO on $SiO_2$ showing a strong absorption at 380 nm.

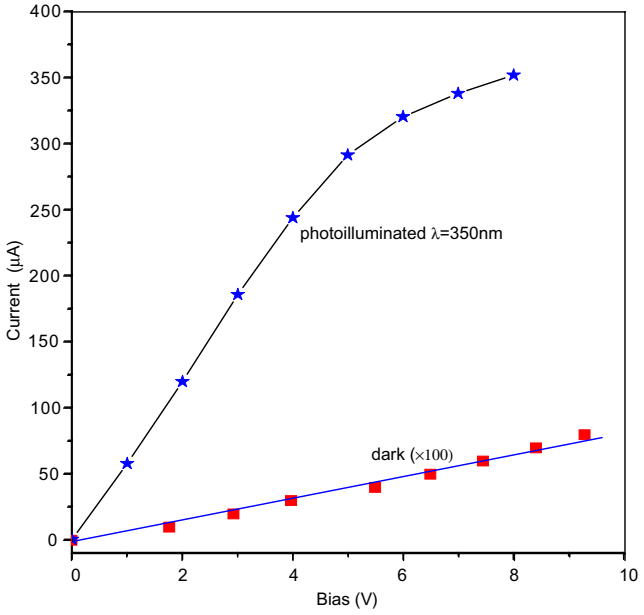


Fig. 4. *I–V* curves show dark current and photocurrent under 350 nm, 1 μW UV light illumination.

ohmic behaviour of Au-electrode on ZnO films contact. Under 3 V bias, the measured average dark current is ~250 nA, which is close to the calculated dark current based on the resistivity of ZnO. This is much smaller compared with Ref. [11]. The low dark current is helpful to enhance the detector's signal to noise (*S*/*N*) ratio since the shot noise, which exceeds the Johnson and 1/*f* noise if the operating frequency is not too low, is proportional to dark current [6]. Upon UV illumination (350 nm, 5 μW) the photocurrent jumped to 300 μA at 5 V bias, indicating a responsivity of ~60 A/W. This responsivity value is a little smaller than that of ZnO prepared by metal organic chemical vapor deposition (400 A/W at 5 V bias,

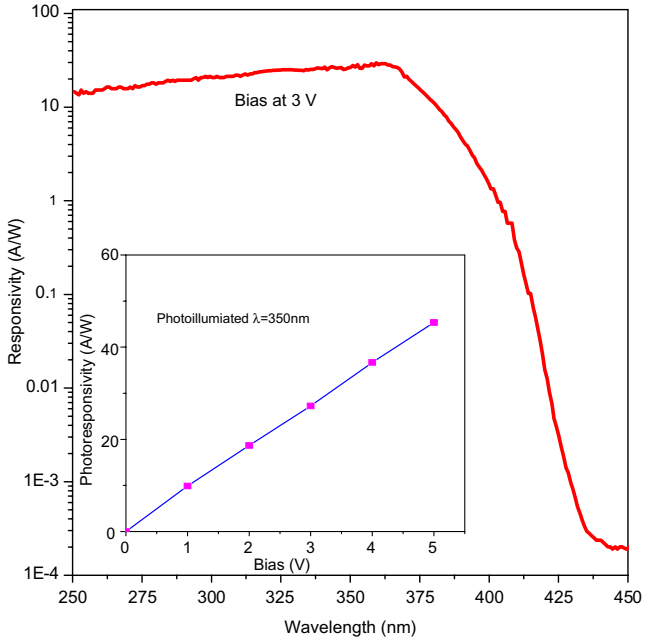


Fig. 5. Spectral response of the ZnO UV detector biased at 3 V. The inset shows the responsivity as a function of bias voltage under 350 nm, 1 μW UV illumination.

2–16 μm interelectrode spacing) photoconductive detectors. Furthermore, it should be noted that the light current did not linearly increase above 5 V applied bias, indicating the sweep-out effect up to this bias [1].

The spectral response of a ZnO UV detector under front illumination is plotted in Fig. 5. Spectral response was performed by a 150 W Xe lamp. A maximum responsivity appeared at 360 nm. In the UV spectral region, the detector showed a high responsivity, with only a little decrease from 360 to 250 nm. The responsivity of a photoconductive detector is generally determined by the quantum efficiency and the photoconductive gain [1]. The maximum responsivity of our detector was measured to be 30 A/W at 360 nm with a 3 V bias. This high responsivity may be attributed to its high photoconductive gain [18]. Meanwhile, it was found that cutoff occurred at around 380 nm (the absorption edge of ZnO). A much broader transition region in between 360 and 420 nm was observed in this figure. This broad transition region also agrees well with the XRD results of ZnO shown in Fig. 2. From the large XRD FWHM and the broad transition region, one can thus conclude that many structure defect induced trap levels indeed exist in the ZnO layer. Meanwhile, it should be noted that the visible rejection (R360 nm/R450 nm) is more than five orders of magnitude, indicating a high degree of visible blindness. The inset of Fig. 5 is the responsivity as a function of bias voltage. A linear relationship was obtained between 1 and 5 V, indicating no carrier mobility saturation or sweep-out effect up to the applied bias. This result is consistent with *I–V* character shown in Fig. 4.

Fig. 6 shows the temporal response of a ZnO UV detector with 3 V bias and 50 Ω load. A pulsed Nd–YAG laser

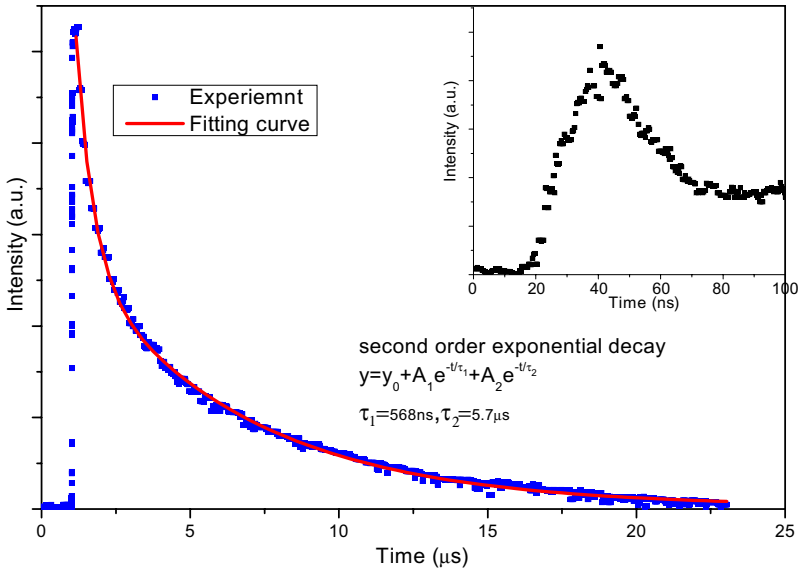


Fig. 6. Temporal response of ZnO UV detectors excited by Nd–YAG laser pulses (355 nm, <10 ns). The inset shows the enlarged impulse response.

(355 nm, 10 ns) was used as the excitation source. The pulse shape in Fig. 6 is strongly asymmetrical: the 20 ns rise time is limited by the excitation laser, which has a nominal pulse duration FWHM 10 ns. The fall time is 10 μs and no persistent photoconductivity was observed. The signal drops to zero at about 25 μs. In order to understand the relaxation mechanism of these devices, exponential fitting have been made to the measured pulse responses. A good second-order fit with time constants of 568 ns and 5.7 μs was obtained for ZnO MSM photodetector, just as shown in Fig. 6. The two time constants used to fit the decay time curves suggest that at least two mechanisms contribute to the slow decay time and it is necessary to consider various physical effects. The RC time constant of the device may have contributed to the slow transient decay. Usually, the photovoltaic detector response time was significantly dominated by the RC time constant of the device duo to the large capacitance of PN junction and Schottky contact. However, RC time constant limit often could be neglected for photoconductive and was confirmed by using different resistances in this letter. Thus the RC limit is ruled out. The transit time limit may be responsible for the slow decay component. The transit time can be expressed as [1]:

$$T_{\mathrm{tr}} = L^2/V\mu_{\mathrm{n}}, \tag{1}$$

where $L$ is the interelectrode spacing, $V$ is applied bias and $\mu_{\mathrm{n}}$ is the electron mobility (estimated 1 $\mathrm{cm}^2$/Vs). At a bias of 3 V, the calculated $T_{\mathrm{tr}}$ is around 80 ns, which may partly contribute 568 ns time constant transient decay. Therefore, there must be other possible factor that can be responsible for this slow decay time other than the transit time. The excess lifetime of trapped carriers may be the most possible reason, especially the trapped holes in n-type semiconductors. It can be confirmed by a large internal gain and a high current responsivity as shown in Fig. 5. The photoresponsivity could be estimated from the equation as [1]:

$$R = q\lambda\eta g/hc, \tag{2}$$

where $\lambda$ is the wavelength, $h$ is Planck's constant, $c$ is the light velocity, $q$ is the electron charge, $\eta$ is quantum efficiency and $g$ is the photoelectric current gain. The photoelectric current gain can be expressed as:

$$g = \tau_{\mathrm{p}}\mu_{\mathrm{n}}V/L^2, \tag{3}$$

where $\tau_{\mathrm{p}}$ is the mean lifetime of holes, $L$ is the interelectrode spacing, $V$ is applied bias and $\mu_{\mathrm{n}}$ is the electron mobility. Assuming the quantum efficiency is unit, we can calculate $\tau_{\mathrm{p}}$ according to Eqs. (2) and (3). The mean lifetime of holes is estimated to be $\tau_{\mathrm{p}} \sim 7$ μs, which is consistent with fitting result of fall time curve (time constant ~5.7 μs). So it can be concluded that the transit time and the excess lifetime of trapped holes may be the main reason for the slow decay time. The origin of trap states may come from the defects in ZnO, or the surface damage during the device processing. Furthermore, the oxygen adsorption at the surface and the grain boundaries of ZnO may also affect the response time [10,19,20].

## 4. Conclusion

In summary, we have demonstrated photoconductive UV detector with MSM structure based on *c*-preferred oriented ZnO film prepared by rf magnetron sputting on quartz substrate. The 200 nm thick Au metal was selected as planar interdigital electrodes. The maximum responsivity of our detector was measured to be 30 A/W at 360 nm with a 3 V bias. The detector shows an ultra fast photoresponse with a rise time of 20 ns. A slow decay time ~10 μs may be mainly caused by the excess life time of trapped holes.

## Acknowledgements

This work is supported by the Key Project of National Natural Science Foundation of China under Grant Nos., 60336020, 50532050, the Innovation Project of Chinese Academy of Sciences. This work is also supported by The National Natural Science Foundation of China under Grant Nos., 60429403, 60376009, 60506014, 50402016 and 60501025.

## References

[1] Razeghi M, Rogalski A. J Appl Phys 1996;79:7433.
[2] Goldberg YA. Semicond Sci Tech 1999;14:R41.
[3] Ohta H, Hosono H. Mater Today 2004;7:42.
[4] Moon TH, Jeong MC, Lee W, Myoung JM. Appl Surf Sci 2005;240:280.
[5] Look DC, Reynolds DC, Hemsky JW, Jones RL, Sizelove JR. Appl Phys Lett 1999;75:811.
[6] Yang W, Vispute RD, Choopun S, Sharma RP, Venkatesan T, Shen H. Appl Phys Lett 2001;78:2787.
[7] Ohtomo A, Kawasaki M, Sakurai Y, Yoshida Y, Koinuma H, Yu P, et al. Mater Sci Eng B 1998;54:24.
[8] Xin-Li Guo H, Tabata T, Kawai. J Cryst Growth 2001;223:135.
[9] Fabricius H, Skettrup T, Bisgaard P. Appl Optics 1986;25:2764.
[10] Liu Y, Gorla CR, Liang S, Emanetoglu N, Lu Y, Shen H, et al. J Electron Mater 2000;29:69.
[11] Xu QA, Zhang JW, Ju KR, Yang XD, Hou X. J Cryst Growth 2006;289:44.
[12] Basak D, Amin G, Mallik B, Paul GK, Sen SK. J Cryst Growth 2003;256:73.
[13] Liang S, Sheng H, Liu Y, Huo Z, Lu Y, Shen H. J Cryst Growth 2001;225:110.
[14] Young SJ, Ji LW, Chang SJ, Su YK. J Cryst Growth 2006;293:43.
[15] Lin TK, Chang SJ, Su YK, Huang BR, Fujita M, Horikosh Y. J Cryst Growth 2005;281:513.
[16] Monroy E, Calle F, Pau JL, et al. J Cryst Growth 2001;230:537.
[17] Monroy E, Calle F, Munoz E, et al. J Electron Mater 1999;28:238.
[18] Munōz E, Monroy E, Garrido JA, Izpura I, Sa'nchez FJ, Sanchez-Garcia MA, et al. Appl Phys Lett 1997;71:870.
[19] Zhang DH. J Phys D 1995;28:1273.
[20] Sharma Parmanand, Sreenivas K. J Appl Phys 2003;93:3693.